# Primary structure of peptides and ion channels

## Role of amino acid side chains in voltage gating of melittin channels

M. T. Tosteson,* O. Alvarez,‡ W. Hubbell,§ R. M. Bieganski,§ C. Attenbach,§ L. H. Caporales,‖ J. J. Levy,‖ R. F. Nutt,‖ M. Rosenblatt,‖ and D. C. Tosteson*

*Laboratory for Membrane Transport, Department of Cellular Molecular Physiology, Harvard Medical School, Boston, Massachusetts 02115; ‡Department of Biology, Faculty of Sciences, University of Chile, Santiago, Chile; §Jules Stein Eye Institute and Department of Chemistry and Biochemistry, University of California at Los Angeles, Los Angeles, California 90024-7008; ‖Merck, Sharp and Dohme Research Laboratories, West Point, Pennsylvania 19486 USA

ABSTRACT Melittin produces a voltage-dependent increase in the conductance of planar lipid bilayers. The conductance increases when the side of the membrane to which melittin has been added (*cis*-side) is made positive. This paper reports observations on the effect of modifying two positively charged amino acid residues within the $NH_2$-terminal region of the molecule: lysine at position 7 (K7), and the $NH_2$-terminal glycine (G1). We have synthesized melittin analogues in which K7 is replaced by asparagine (K7-N), G1 is blocked by a formyl group (G1-f), and in which both modifications of the parent compound were introduced (G1-f, K7-N). The time required to reach peak conductance during a constant voltage pulse was shorter in membranes exposed to the analogues than in membranes modified by melittin. The apparent number of monomers producing a conducting unit for [K7-N]-melittin and [G1-f]-melittin, eight, was found to be greater than the one for [G1-f], K7-N]-melittin and for melittin itself, four. The apparent gating charge per monomer was less for the analogues, 0.5–0.3 than for melittin, one. Essentially similar results were obtained with melittin analogues in which the charge on K7 or G1 or both was blocked by an uncharged *N*-linked spin label. These results show that the positive charges in the $NH_2$-terminal region of melittin play a major but not exclusive role in the voltage gating of melittin channels in bilayers.

## INTRODUCTION

Melittin, the main component of bee venom, is a polypeptide which comprises 26 amino acid residues including five with positively charged side chains in addition to the $NH_2$-terminal glycine (1). This peptide has been found to increase the permeability of biological membranes to ions and other small, hydrophilic molecules (1) to produce cell lysis (2, 3) and to form voltage-gated channels in lipid bilayers (4, 5). The conductance induced in bilayers by melittin is anion selective and displays first activation and then inactivation during a constant voltage pulse. From the concentration and voltage dependence of the peak conductance it is possible to infer the apparent number of melittin monomers per conducting unit, 4, and the apparent gating charge per conducting unit, +4(4). Apparently, monomers of the peptide interact with each other and with the phospholipids in the lipid bilayers to produce pathways through which ions can move. A plausible model for the increase in membrane permeability induced by melittin is that the amphiphilic helices of melittin (6, 7) aggregate so that their hydrophilic faces line the walls of the channel while the hydrophobic faces interact with the hydrocarbon chains of the phospholipids. A similar role has been proposed for the amphiphilic helical segments of channel forming proteins in biological membranes (8).

Because melittin molecules have a high dipole moment (9), their interaction with a positive voltage applied to the side where the peptide has been added would tend to push the $NH_2$-terminal end through the membrane and increase the probability of finding a melittin molecule spanning the bilayer. This implies the energetically unfavorable movement of the charges at G1 and K7 through the low–dielectric constant of the membrane, which would limit the number of channels formed in the membrane. If this model is correct, melittin analogues, in which the charged residues at G1 and K7 are neutralized, should form channels more readily than melittin. To test this hypothesis, we synthesized analogues in which the glycine at position 1 was blocked with a formyl group (G1-f), the lysine at position 7 was replaced by asparagine (K7-N), and in which both residues were so altered (G1-f, K7-N). We also prepared derivatives of melittin in which spin labels were attached to either G1 or K7 or to both simultaneously. We then compared the electrical properties of bilayers exposed to one of these compounds or to melittin. We chose to study in detail the conductance of membranes containing many channels induced by melittin and its analogues, because the single channels induced by these compounds are heterogeneous in amplitude and duration as the voltage is changed, properties which are difficult to interpret in terms of a relatively simple model (10, 11, and Tosteson, M. T., personal observations).

## MATERIALS AND METHODS

### Materials

Asolectin was purchased from Associated Concentrates (Woodside, NY) and squalene from Kodak Laboratory and Specialty Chemicals,


0006-3495/90/12/1367/09 $2.00

Eastman Kodak Co., (Rochester, NY). All other chemicals were analytical grade and were purchased from Baxter Healthcare Co. (Pittsburgh, PA) and Aldrich Chemical Co. (Milwaukee, WI). Stock solutions of melittin and its analogues were made in 95% ethanol and kept at −50°C at a concentration of 3 mM. Substock solutions were prepared fresh daily.

## Peptide synthesis

The structure of the peptides synthesized: melittin, [Asn$^7$]-melittin, *N*-α-formylmelittin, and [Asn$^7$, *N*-α-formyl]-melittin is shown in Table 1. These peptides were synthesized by the solid phase method of Merrifield (12) on an Applied Biosystems Inc., model 430A (Foster City, CA) automated peptide synthesizer utilizing a para-methylbenzhydrylamine resin as the solid support. t-Boc was used for *N*-α protection. The methods utilized have been reported previously (13, 14). Peptide cleavage was accomplished using the "low-high" procedure of Tam et al. (15). The *N*-α-formylmelittin peptide was prepared by coupling *N*-α-formyl glycine (Sigma Chemical Co., St. Louis) as a preformed symmetrical anhydride generated from *N*-α-formyl glycine and *N*,*N*'-dicyclohexyl carbodiimide. The peptides were purified by preparative reversed-phase HPLC with a linear gradient of 30–45% 0.1% TFA in $CH_3CN$. The fractions containing the peak were then analyzed by HPLC on a Vydac $C_4$ column (Separations Group, Hesperia CA). The purest fractions were then pooled and lyophilized. The purity of the samples (>99.5%) was determined by NMR spectroscopy, fast atom bombardment mass spectrometry (FABMS), and amino acid composition.

## Spin-labeled melittin

The spin-labeled derivatives of melittin were obtained by a partial reaction of the amino group with succinimidyl-2,2,5,5-tetramethyl-3-pyrroline-1-oxyl-3-carboxylate as previously described (16). The purification steps were modified as follows: (*a*) phosphoric acid concentration was reduced from 0.1% to 0.01%; (*b*) desalting was done on a polymeric reversed phase column (Model PRO-3; Hamilton Co., Reno NV) using a water to $CH_3CN$ gradient in 0.1% TFA.

## Lipid bilayers

Bilayers were made from aposition of two monolayers spread from a solution of asolectin dissolved in pentane (20 mg/ml) as previously described (1). The aqueous solutions contained 0.5 M $NaNO_3$ ($KNO_3$) (pH 6, room temperature) and were stirred with magnetic stirrers. The partitions were punched to have a membrane capacitance of 150 (±20) pF (giving a calculated area of ~$1.8 \times 10^{-4}$ cm$^2$) for all experiments reported in this paper.

## Electrical measurements

Recordings of the steady-state membrane current were performed using a 3900 patch-clamp amplifier (DAGAN Corp., Minneapolis MN) and begun one hour after addition of the various peptides to the aqueous phase, to insure the reproducibility of the conductance measurements. Holding potential corresponds to the potential applied to the *cis*-chamber using silver–silver electrodes connected to the solutions via salt bridges (2.5% agar in the chamber medium, electrodes immersed in 1 M KCl). Holding potentials and pulse protocols were generated using Indec's "Box-basic-fastlab" with a 40-MHz Labmaster A/D board (Tecmar Inc., Cleveland, OH) and OPTO isolation to the D/A converter (Indec, Sunnyvale, CA) together with a 25 MHz, 286-based computer (Dell Computer Co., Austin, TX). The same unit was also used to digitize and average pulses on line.

## Pulse protocol

The pulse sequence used at each holding potential is shown in Fig. 1. The initial current was determined by applying 20 pulses of amplitude $V_h$, duration 50–100 ms, and rate of 3–6 Hz (*A*). This was followed by one pulse of sufficient duration (30–60 s) to attain steady state (*B*) and determine both peak and steady-state current. Once in the steady state, the determination of the slope current was made as indicated in (*C*), by applying a test pulse pattern in which each step was applied 5–10 times and had a duration of 200–300 ms and an increasing amplitude from 20–40 mV negative to the holding potential to a total of 20–50 mV positive to the holding potential, in steps of 5 mV. At the end of each complete run, recovery from the steady state was obtained by leaving the membrane for 15 min at 0 mV.

## Conductance determination

The initial conductance was determined by extrapolation of the single exponential fit of the first 20 ms of the resulting averaged current curves (obtained with pulse protocol *A*, and Fig. 1). The slope conductance ($G_{ins}$) was calculated by taking the value of the current at 200 ms from the curves obtained using the test pulse protocol (*C*) and dividing by ($V_t - V_h$). The dependence of the peak conductance ($G_p$) and of the steady-state (chord) conductance ($G_{ich}$) on concentration and voltage were determined as previously described (4). Data were fit to the

**TABLE 1. Sequence of synthetic peptides**

Melittin
$H_3N$ G—I—G—A—V—L—K—V—L—T—T—G—L—P—A—L—I—S—W—I—K—R—K—R—Q—Q—$CONH_2$
1 7 14 21

*N*-α-formylmelittin (G1-f)
Formyl G—I—G—A—V—L—K—V—L—T—T—G—L—P—A—L—I—S—W—I—K—R—K—R—Q—Q—$CONH_2$
1 7 14 21

[Asn$^7$]-melittin] (K7-N)
$H_3N$ G—I—G—A—V—L—N—V—L—T—T—G—L—P—A—L—I—S—W—I—K—R—K—R—Q—Q—$CONH_2$
1 7 14 21

[Asn$^7$, *N*-α-formyl]-melittin (G1-f,K7-N)
Formyl G—I—G—A—V—L—N—V—L—T—T—G—L—P—A—L—I—S—W—I—K—R—K—R—Q—Q—$CONH_2$
1 7 14 21

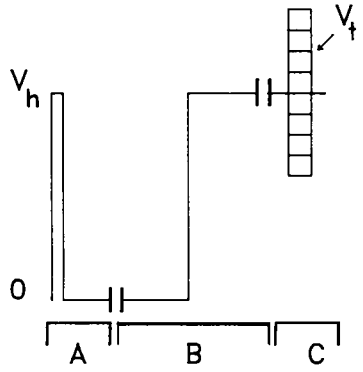


FIGURE 1 Voltage pulse protocol. *A*: initial current determination; duration 50–100 ms, repeated 20 times; *B*: the approach to steady state; duration 30 s (or longer) followed by *C*: determination of slope conductance of steady state; duration 200 ms. $V_h$: holding potential; $V_t$: test pulse: in *C* $V_t$ varies ± 20 or ± 50 mV from $V_h$, beginning from the pulses negative to the holding potential.

equation: $G_x = [\text{peptide}]^m (\exp neV/kT)$, where $e$ is the electronic charge, $k$ is the Boltzmann constant, $T$ is the temperature, and $m$ and $n$ are empirical constants which describe the dependence of the conductance on the concentration of the peptide in the aqueous phases ([peptide]) and on the applied voltage ($V$). In some instances, the values of the initial conductance and of the steady-state conductance were normalized to the value of the peak conductance, taken as a measure of the maximum number of conducting units open at a given peptide concentration and voltage. In these cases, the values of the conductances had been measured during the same run, after the complete protocol as indicated in Fig. 1.

## RESULTS

### Effects of charge removal on the time-dependent conductance

The data summarized in the figures address the influence of positively charged residues at the $NH_2$-terminal region on voltage gating and other properties of the conductance that melittin induces in phospholipid bilayers. Fig. 2 shows the time course of membrane conductance during the interval when the membrane potential is maintained at a constant value (Fig. 1 *B*). As described previously for melittin (4), the conductance does not remain constant at a given membrane potential, but, rather, first activates and then inactivates. For purposes of comparison, we identify three values of the conductance: $G_0$, $G_p$, and $G_i$, and two values of time: $t_p$ and $\tau$(inactivation). $G_0$ is the conductance at the time when the voltage pulse is imposed, $G_p$ is the peak conductance, and $G_i$ is the steady-state conductance that persists after inactivation is complete. $t_p$ is the time to peak and $\tau$(inactivation) is the time constant for inactivation.

Fig. 2 *a* compares melittin with analogues in which the $NH_2$-terminal glycine is blocked by a formyl group (G1-f) or by a spin label (G1-1b). The values of peptide concentration and membrane potential were chosen so as to produce approximately the same peak conductance for all three compounds. The most striking difference between the behavior of membranes containing melittin and those containing the analogues in which the $NH_2$-terminal glycine is blocked is that the time to peak is substantially shorter for the analogues. We have shown previously (5) that the conductance in membranes containing melittin displays an early rapid rise to a plateau and subsequent slower activation to the peak conductance. The early plateau is not evident in membranes exposed to the analogues. The extent and rate of inactivation is about the same for melittin and for these two analogues as shown in Fig. 2 *a* (cf also Fig. 6 *a*).

Essentially similar results were obtained when bilayers were exposed to analogues in which the lysine at position 7 was replaced by asparagine (K7-N), or blocked by a spin label (K7-1b), as well as with compounds that were altered at both the $NH_2$-terminal glycine and at lysine 7 (G1-f, K7-N and G1-1b, K7-1b) (cf Fig. 2, *b* and *c*). In all four cases, time to peak was significantly shorter than with melittin, the onset of inactivation occurred earlier and the activation was less sigmoid. Apparently, the slow onset of activation of melittin requires the presence of positively charged residues at both positions 1 and 7 of the peptide.

As is evident in Fig. 2, we found that the electrical properties were the same in membranes exposed to melittin analogues in which the charged amino group at position 7 was removed in two different ways; by amino acid substitution (e.g., K7-N) or by reaction of the $\epsilon$-amino group of lysine 7 with a spin label (K7-1b). Likewise, there was no difference in the effect of analogues with the charge at position 1 removed by reaction of the terminal glycine amino group with a formyl or a spin label group. These results strongly support the notion that it is the removal of charge rather than some steric effect of blocking or amino acid substitution that is responsible for the difference in the behavior of melittin and its analogues. In the following figures, then, we will not make a distinction in reporting the results obtained when bilayers were exposed to analogues with the charge removed at position 1 or 7 by either mechanism, which will be designated G1 (or K7). Results using analogues with no charge at both positions are designated G1K7.

### Effect of charge removal on the kinetics of activation and inactivation

Fig. 3 *a* shows in more detail the effects of altering the amino acids at positions 1 and 7 of melittin on the kinetics

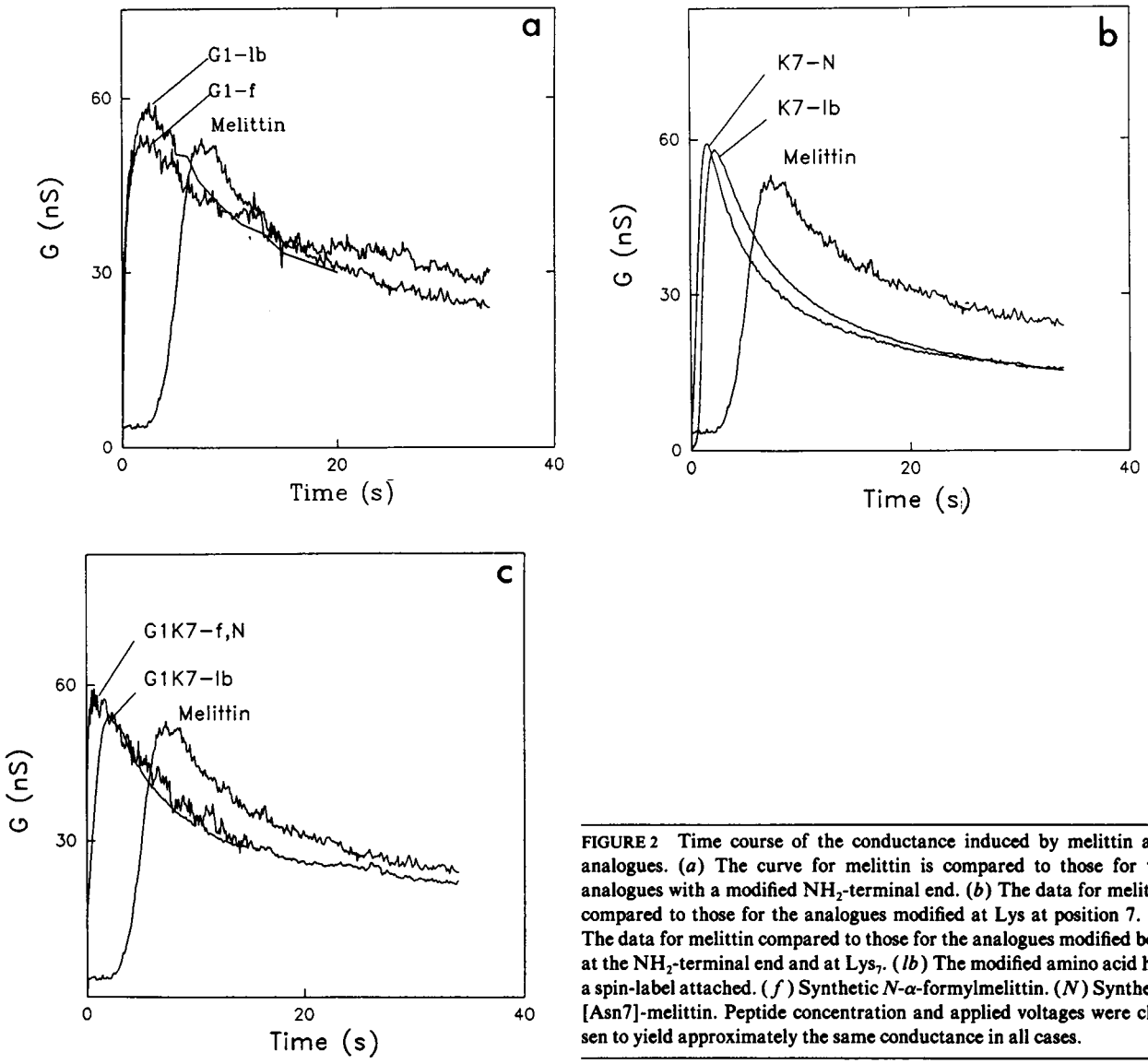


FIGURE 2 Time course of the conductance induced by melittin and analogues. (*a*) The curve for melittin is compared to those for the analogues with a modified $NH_2$-terminal end. (*b*) The data for melittin compared to those for the analogues modified at Lys at position 7. (*c*) The data for melittin compared to those for the analogues modified both at the $NH_2$-terminal end and at $Lys_7$. (*Ib*) The modified amino acid had a spin-label attached. (*f*) Synthetic *N*-α-formylmelittin. (*N*) Synthetic [Asn7]-melittin. Peptide concentration and applied voltages were chosen to yield approximately the same conductance in all cases.

of the current response during voltage clamping of bilayers exposed to these peptides. The time to peak ($t_p$) is substantially shorter for all of the analogues tested compared to melittin (cf Fig. 3 *a*). The difference becomes more pronounced as the magnitude of $G_p$ is increased either by increasing the voltage or the peptide concentration. $t_p$ is shorter for G1 than for K7 compounds. Apparently, the charges at the $NH_2$-terminus of the peptides slow the process of peptide monomers arranging themselves in the membrane to form conducting units and thus slow down the time of onset of activation.

Fig. 3 *b* shows the effect of altering the primary structure of melittin on the time constant for inactivation of conductance $\tau$ (inactivation) in membranes exposed to melittin or its analogues. Apparently the charges at G1 and K7 do not affect the rate constant for the process once it has begun.

## Effect of charge removal on the peak conductance, $G_p$

Fig. 4 *a* shows the dependence of the peak conductance, $G_p$, on the concentration of melittin or its analogues. As shown previously, $G_p$ depends on the fourth power of the melittin concentration (4) suggesting that the conducting unit is tetrameric. Reducing the $NH_2$-terminal charge by blocking or substitution at position 1 or at position 7 substantially increases the aggregation numbers to 8 or 9. Suprisingly, elimination of charges at both positions 1 and

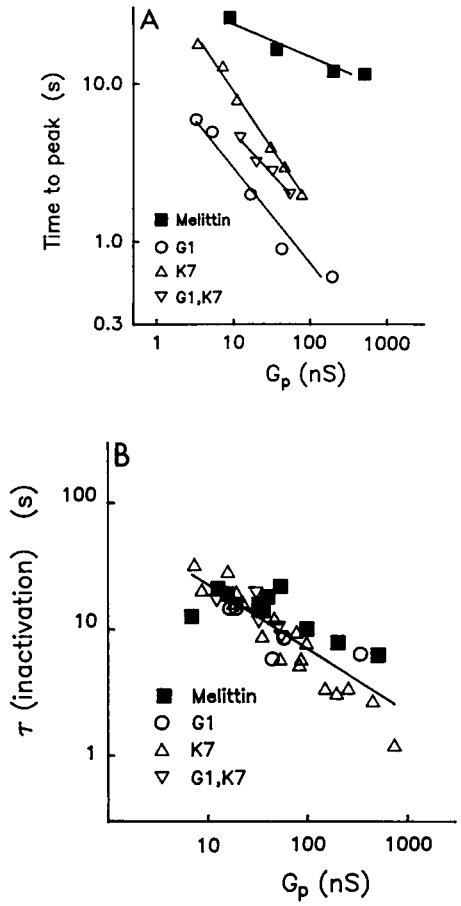


FIGURE 3 Kinetics of conductance activation (*A*) and inactivation (*B*). In (*A*), the log of the total time taken to reach the peak conductance ($t_p$) and in (*B*), the rate constant for inactivation ($\tau_{(inactivation)}$), in logarithmic scale, are plotted as a function of the log of the peak conductance ($G_p$)

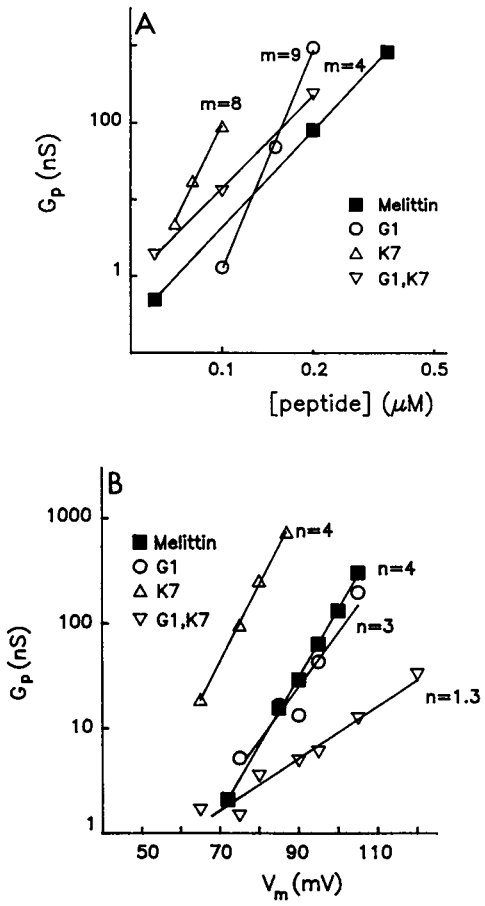


FIGURE 4 Dependence of the peak conductance on the concentration of melittin and analogues (*A*) and voltage (B). The peak conductance ($G_p$) and the steady state, chord conductance ($G_{ich}$) were determined using protocol B (Fig. 1). Further experimental details are described in the section Materials and Methods.

7 produces no change in the aggregation number compared to melittin.

Fig. 4 *b* shows the voltage dependence of $G_p$. As reported previously for melittin, the apparent gating charge for the units that produce $G_p$ is 4, or one charge per monomer of the tetramer. The apparent gating charge for the conducting units of G1 and K7 is also 4. However, because the apparent aggregation number for these peptides is about 8, the apparent gating charge per monomer is about 0.5. The apparent gating charge for the analogue with charges at neither residue 1 nor residue 7 (G1K7) is 1.3, yielding an apparent gating charge per monomer of 0.3. Apparently, the voltage dependence of the peak conductance induced by melittin in bilayers is strongly dependent on the magnitude of the positive charge residing at or near the $NH_2$-terminus of the peptide.

## Effect of charge removal on the initial conductance

Fig. 5 shows the effect of altering the charges at the $NH_2$-terminal end of melittin on the initial conductance, $G_0$, relative to the conductance at the peak, $G_p$. The figure shows that, as is the case for melittin, the analogues induce an initial conductance in the lipid bilayers, the one exception being the analogue in which the positive charge was removed at position 7, K7.

## Effect of charge removal on the steady-state conductance, $G_1$

Fig. 6 *a* shows the conductance of the steady state after inactivation $G_{ich}$, as a function of the peptide concentration. $G_{ich}$ was found to be practically independent of

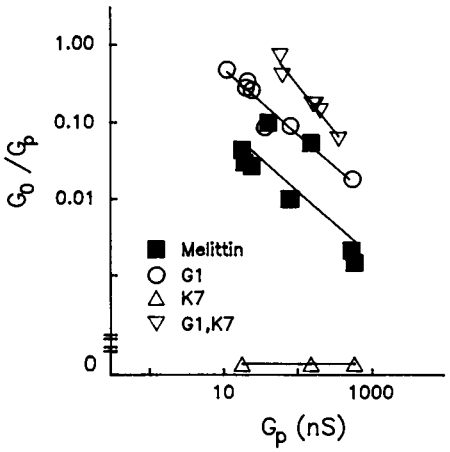


FIGURE 5 The initial conductance induced by melittin and analogues. Double logarithmic plot of the ratio of the initial conductance ($G_0$) to the peak conductance ($G_p$) as a function of $G_p$. $G_0$ was obtained by extrapolation from an exponential fit of the first 20 ms of the current response to a voltage pulse as detailed in region *A* of Fig. 1. The results were obtained on several membranes, at different peptide concentrations.

concentration for melittin but not for the analogues. In contrast, as shown in Fig. 6 *b*, the voltage dependence of this residual conducting unit is low and the same for all the compounds, including melittin, suggesting that the positive charges near the $NH_2$-terminal region are not important in determining the voltage dependence of $G_{ich}$.

Fig. 7, shows the extent of inactivation, measured as the ratio of $G_{ich}$ to $G_p$, is the same for all compounds tested. $G_p$ was increased by a combination of increasing the membrane potential and the amount of melittin or its analogues in the membrane. There was no significant difference between the behavior of membranes exposed to the parent compound, melittin and to all the analogues.

Fig. 8 shows the results of experiments in which the chord conductance of the membrane after inactivation, $G_{ich}$, is compared with the slope conductance measured ($G_{iss}$) after the protocol indicated in Fig. 1, *C*. When the test pulses were 50 mV (or more) negative to the holding potential, there was no significant difference between the chord and slope conductances for melittin or for any of the analogues tested (not shown). However, when the test potentials were closer to or positive from the holding potential, activation of the steady-state conductance occurred. The magnitude of the voltage activation of the steady-state conductance was greater for K7 and for G1 than for G1K7 and melittin itself, which suggest that this apparent activation of the steady state might be due to new conducting units inserting into the bilayer.

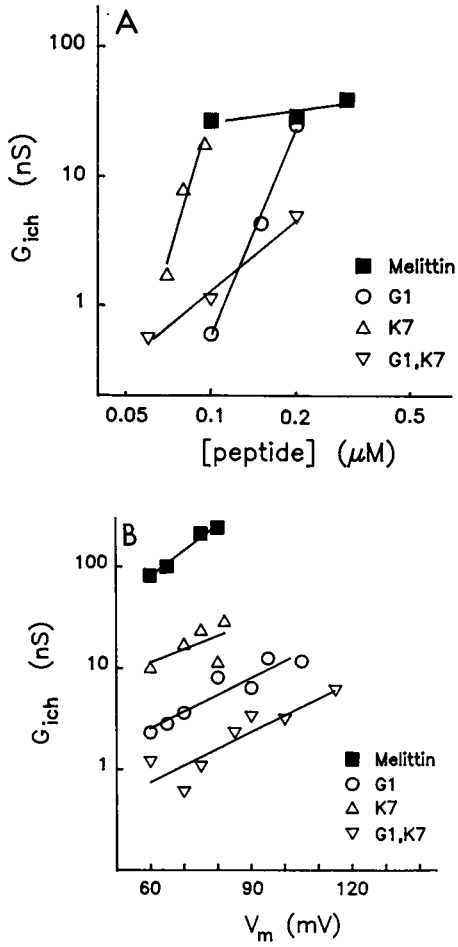


FIGURE 6 Dependence of the steady state conductance $G_{ich}$ on peptide concentration (*A*) and (*B*) on voltage ($V_m$) (*B*). Experimental details as in Fig. 4.

## DISCUSSION

Several peptides other than melittin have been shown to aggregate and produce channels in bilayers. Some of these form channels in a way that is independent of voltage (17, 18), whereas others are voltage gated (19–21). All of these peptides can form helices that are amphipathic, that is, one side of the helix displays side chains that contain hydrophilic groups, whereas the opposite side exhibits hydrophobic side chains (22). These compounds are surface active and frequently lytic. It is reasonable to suppose that such monomers can form oligomers with their hydrophilic groups lining the walls of a channel while their hydrophobic groups interact with the aliphatic chains of adjacent phospholipids.

The mechanism of voltage gating of such channels is

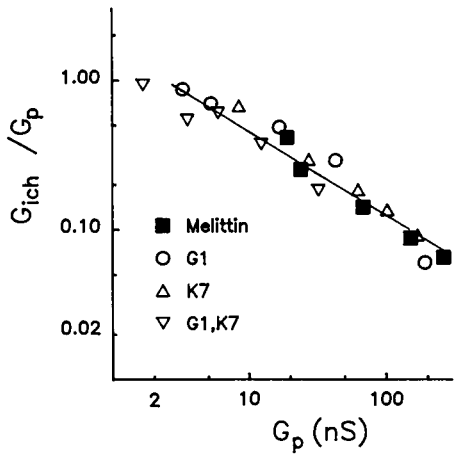


FIGURE 7 Dependence of the extent of inactivation ($G_{ich}/G_p$) on the peak conductance ($G_p$). Experimental details as in Fig. 4.

obscure. Some have suggested that the helical dipole moment of the peptide chains lining the channel is a decisive determinant (23). It has also been argued that bound ions could supply the gating charge (24). Others have emphasized the potential role of charged groups on the side chains of the peptides (25). The data presented in this paper support the view that charged groups on side chains can, directly or indirectly, contribute to the gating charge of peptide channels.

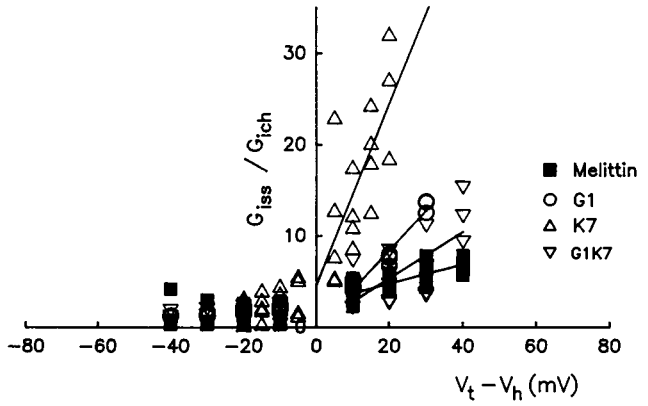


FIGURE 8 The slope conductance ($G_{iss}$) of the steady state. The slope conductance of the steady state was obtained with protocols B and C of Fig. 1. The test pulses ($V_t$) were of 200 ms duration. The maximum change from the holding potential ($V_h$) was 40 mV. The value of $G_{iss}$ was calculated either from the exponential fit to the current responses to the various ($V_t$–$V_h$) applied (in the cases where the current was activated) or from the value of the current at 200 ms. The points shown at each value of $V_t$–$V_h$ correspond to different values of $V_h$, obtained in one membrane exposed to a specific peptide.

We made use of two different methods of removing charge from melittin. The size of the side-chains introduced was different in the two methods. Nevertheless, we found that the actions of the analogues were the same irrespective of the method of charge removal (e.g., substitution of asparagine for lysine at position 7 as compared with blockage of the $\epsilon$-amino group of lysine by a bulky spin label). We infer that the effects observed were due to charge removal rather than to steric factors per se.

We will discuss our results within the framework of a hypothetical, qualitative model of the action of melittin and its analogues on the ionic permeability of lipid bilayers. Some of the steps in the model are voltage independent and some are voltage dependent.

## Voltage independent steps

(Step *1*) Melittin monomers in random coil conformation adsorb onto the surface of the bilayer (16). (Step *2*) Monomers on the membrane surface slowly change shape to become $\alpha$-helices (26). (Step *3*) Helical monomers, with the hydrophilic faces of the helices directed toward the aqueous solution while the hydrophobic faces are directed toward the interior of the membrane aggregate to form dimers. A few of these dimers enter the membrane in such a way as to produce a small increase in membrane conductance in the absence of an externally applied electrical field as revealed in the conductance measured at the beginning of a pulse ($G_0$) (5). The combination of these steps requires many minutes and accounts for the long time of exposure to melittin required before the characteristic conductance changes are observed.

## When a *cis*-positive voltage is applied

(Step *4*) The $NH_2$-terminal end of dimers (and monomers) move toward the *trans*-side of the membrane under the influence of the electrical field so that the axes of the $\alpha$-helices become more perpendicular to the surface of the membrane. The charges at the $NH_2$-terminal region in the melittin molecule make this process energetically unfavorable and slow (cf. Figs. 2 and 3).

(Step *5*) The dimers (and monomers) that have reoriented in the membrane aggregate to form conducting channels accounting for the sigmoidal increase in conductance shown in Fig. 2. The number of such channel-forming aggregates is a small fraction of the total number of peptide molecules located at the membrane surface, as has been found to be the case for other reconstituted peptides and proteins (27).

(Step *6*) The conductance of the membrane falls from

its peak value either by a reduction in the total number of open channels and/or by a decrease in the unit conductance of each open channel. These changes may result from partial blockage of channels by melittin monomers or by penetrating ions. Alternatively, the quaternary structure of the melittin aggregate may undergo some slow change in the electric field which leads to the reduced conductance. The peak conductance occurs when the rates of formation and inactivation of channels are equal.

In terms of this picture of melittin interaction with the membrane, it is apparent that the amino groups at the $NH_2$-terminal glycine and on the side chain of lysine-7 are involved in steps *4* and *5*, leading to the formation of conducting tetramers. As the results shown in Fig. 2 and 3 indicate, the presence of charges at positions 1 and 7 lengthens the time required to reach the peak conductance (steps *4* and *5*) but not the time constant for inactivation (step *6*). Step 4 involves the change in orientation of the melittin monomers, which in turn involves the movement of the two positive charges across the membrane, a process with an activation energy of 50–80 Kcal/mol. An alternative is that the melittin molecule loses a proton and tilts in an uncharged form, becoming reprotonated as the basic residues reach the *trans*-side. This process has a probability of 1/16,000, therefore, the process is slow. If one of the charges is eliminated permanently, the process would be 16,000 times faster and 250,000 times faster if both charges are absent (cf. Figs. 2 *c* and 5). As the positive charge on the $NH_2$-terminal region of the melittin molecule is reduced, step 4 would be less voltage-dependent, but not independent of voltage because the large $\alpha$-helical dipole moment of melittin persists in the absence of the charged $NH_2$-terminus and the side chain at position 7. Apparently the charges at positions 1 and 7 do not influence the rate of step 6. From the evidence available at this time, it is not possible to specify how the charges at positions 1 and 7 are involved in oligomerization of melittin, but they do seem to limit the extent of the reaction to tetramers, and to make the process more sensitive to voltage.

From the physiological point of view, it is interesting to speculate about the relevance of channels formed by the aggregation of relatively small peptides like melittin to the channels formed by integral membrane proteins such as the voltage-gated sodium channel or the ligand-gated acetyl choline channel. In this regard, it is noteworthy that all channel proteins that have thus far been sequenced contain several putative intramembrane helical segments that are either hydrophobic or amphipathic. Although the detailed, three-dimensional structure of these proteins has yet to be elucidated by x-ray crystallography, many investigators have speculated that the amphipathic segments form the walls of the channels. It is reasonable to suppose that there are fewer degrees of freedom in the structure of such intraprotein channels than in the channels formed by oligomerization of peptides that are not covalently linked. According to this view, an important function of the nonchannel forming parts of biological membrane channel proteins is to constrain the structure of the channel within physiologically tolerable limits. Absent such constraints, melittin and other small peptides are free to form a greater variety of electrically conducting molecular arrangements.

We would like to thank J. A. Halperin and R. MacKinnon for helpful comments on the manuscript.

This work was supported in part by National Institutes of Health grant GM 25277 (MTT).

*Received for publication 31 May 1990 and in final form 1 August 1990.*

## REFERENCES

1. Habermann, E. 1972. Bee and wasp venoms. *Science (Wash. DC.).* 177:314–322.
2. DeGrado, W. F., G. F. Musso, M. Lieber, E. T. Kaiser, and F. J. Kezdy. 1982. Kinetics and the mechanism of hemolysis induced by melittin and by a synthetic melittin analogue. *Biophys. J.* 37:329–338.
3. Tosteson, M. T., S. J. Holmes, M. Razin, and D. C. Tosteson. 1985. Melittin lysis of red cells. *J. Membr. Biol.* 87:35–44.
4. Tosteson, M. T., and D. C. Tosteson. 1981. The sting: melittin forms channels in lipid bilayers. *Biophys. J.* 36:109–116.
5. Tosteson, M. T., and D. C. Tosteson. 1984. Activation and inactivation of melittin channels. *Biophys. J.* 45:112–114.
6. Eisenberg, D., T. C. Terwilliger, and F. Tsui. 1980. Structural studies of bee melittin. *Biophys. J.* 32:252–254.
7. Bazzo, R., M. J. Tappin, A. Pastore, T. S. Harvey, J. A. Carver, and I. D. Campbell. 1988. The structure of melittin. A $^1$H-NMR study in methanol. *Eur. J. Biochem.* 173:139–146.
8. Eisenberg, D., E. Schwarz, M. Komaromy, and R. Wall. 1984. Analysis of membrane and surface protein sequences with the hydrophobic moment plot. *J. Mol. Biol.* 179:125–142.
9. Sano, T., and G. Schwarz. 1983. Structure and dipole moment of melittin molecules in butanol/water as derived from dielectric dispersion and circular dichroism. *Biochim. Biophys. Acta.* 745: 189–193.
10. Tosteson, M. T., O. Alvarez, and D. C. Tosteson. 1985. Peptides as promoters of ion-permeable channels. *Regul. Pept. Suppl.* 4:39–45.
11. Hanke, W., C. Methfessel, H.-U. Wilmsen, E. Katz, G. Jung, and G. Boheim. 1983. Melittin and a chemically modified trichotoxin form alamethicin-type multi-state pores. *Biochim. Biophys. Acta.* 727:108–114.
12. Barany, G., and B. M. Merrifield. 1980. *In* The Peptides. E. Gross and J. Meienhofer, editors. Vol. 2. Academic Press Inc., N.Y. 1–284.
13. Tosteson, M. T., J. J. Levy, L. H.Caporale, M. Rosenblatt, and D. C. Tosteson. 1987. Solid phase synthesis of melittin: purifica-

tion and functional characterization. *Biochemistry.* 26:6627–6631.

14. Caporale, L., R. Nutt, J. J. Levy, J. Smith, B. Arison, C. Bennett, G. Albers-Schonberg, S. Pitzenberger, M. Rosenblatt, and R. Hirschnann. 1989. Characterization of synthetic parathyroid hormone analogues and of synthetic byproducts. *J. Org. Chem.* 54:343–346.
15. Tam, J., W. Heath, and R. B. Merrifield. 1983. $S_N2$ deprotection of synthetic peptides with a low concentration of HF in dimethyl sulfide: evidence and application in peptide synthesis. *J. Am. Chem. Soc.* 105:6442–6445.
16. Altenbach C., and W. L. Hubbell. 1988. The aggregation state of spin-labeled melittin in solution and bound to phospholipid membranes: evidence that membrane-bound melittin is monomeric. *Proteins Struct. Funct. Genet.* 3:230–242.
17. Andersen, O. S. 1984. Gramicidin channels. *Annu. Rev. Physiol.* 46:531–548.
18. Oiki, S., W. Danho, and M. Montal. 1988. Channel protein engineering: synthetic 22-mer peptide from the primary structure of the voltage-sensitive sodium channel forms channels in lipid bilayers. *Proc. Natl. Acad. Sci. USA.* 85:3534–3539.
19. Eisenberg, M. J., J. E. Hall, and C. A. Mead. 1973. The nature of the voltage-dependent conductance induced by alamethicin in black lipid membranes. *J. Membr. Biol.* 14:143–176.
20. Menestrina, F., K. P. Voges, G. Jung, and G. Boheim. 1986. Voltage-dependent channel formation by rods of helical polypeptides. *J. Membr. Biol.* 93:111–132.
21. Tosteson, M. T., D. S. Auld, and D. C. Tosteson. 1989. Voltage-gated channels formed in lipid bilayers by a positively charged segment of the Na-channel polypeptide. *Proc. Natl. Acad. Sci. USA.* 86:707–710.
22. Eisenberg, D. 1984. Three dimensional structure of membrane and surface proteins. *Annu. Rev. Biochem.* 53:595–623.
23. Hall, J. E., I. Vodyanoy, T. M Balasubramanian, and G. R. Marshall. 1984. Alamethicin: a rich model for channel behavior. *Biophys. J.* 45:233–247.
24. Andersen, O. S., and R. U. Muller. 1982. Monazomycin-induced single channels: I. Characterization of the elementary conductance events. *J. Gen. Physiol.* 80:403–426.
25. Honig, B. H., W. L. Hubell, and R. F. Flewelling. 1986. Electrostatic interactions in membranes and proteins. *Annu. Rev. Biophys. Chem.* 15:163–193.
26. Schwarz, G., and G. Beschiaschvili. 1989. Thermodynamic and kinetic studies on the association of melittin with a phospholipid bilayer. *Biochim. Biophys. Acta.* 979:82–90.
27. Tosteson, M. T. 1978. Interaction between a membrane sialoglycoprotein and planar lipid bilayers. *J. Membr. Biol.* 38:291–309.